JOURNAL OF MATERIALS SCIENCE 9 (1974) 2034–2051

Review

Deformation mechanisms in crystalline polymers

P. B. BOWDEN*, R. J. YOUNG†
Department of Metallurgy and Materials Science, University of Cambridge, UK

The mechanisms which have been suggested to explain the deformation of crystalline polymers are reviewed. Emphasis has been placed upon the type of information that can be gained from experimental observations and on the extent to which those observations are consistent with suggested deformation mechanisms and current ideas on polymer structure and morphology.

1. Introduction

During the last few years a great deal of work has been published on both experimental and theoretical aspects of deformation mechanisms in crystalline polymers. In this review we have attempted to summarize the present state of knowledge in the area, laying particular emphasis on the type of information that can be obtained from experimental observations and on the degree to which experimental observations have been able to substantiate theoretical predictions.

The subject has been reviewed by Peterlin [1] and by Kambour and Robertson [2]. Since these reviews were written advances in the understanding of polymer morphology and the preparation of materials with better textures has enabled more precise information to be obtained.

We have been primarily concerned with deformation processes occurring at intermediate strains. Relaxation effects in crystalline polymers have been reviewed by McCrum *et al.* [3] and processes occurring at large strains during drawing have been considered by Peterlin [4]. We have not attempted to cover either topic in this review.

2. Elastic moduli

Work on the elastic moduli of polymers has been reviewed recently [5] and only the particular points relevant to the deformation of polymer crystals will be summarized here. We are concerned of course with the elastic moduli of the crystals themselves rather than moduli of bulk samples of the polymer.

Polymer crystals are highly anisotropic and for crystals of the lowest symmetry (triclinic) 21 independent constants are needed to fully define their elastic properties. For crystals of higher symmetry the number is reduced, being 13 for monoclinic, 9 for orthorhombic and 5 for hexagonal crystals. An excellent introduction to anisotropic elasticity is given in Chapter five of [6].

The two principal techniques for determining polymer crystal moduli are X-ray measurements under stress [7] and inelastic neutron scattering [8]. At the present time a complete set of elastic constants has not been determined experimentally for any polymer although for PE such a set has been calculated [9]. The elastic constants that have been determined experimentally are primarily those associated with tensile deformations (S_{11}, S_{22}, S_{33}) rather than those that determine the shear deformation of a crystal in response to a shear stress (S_{44}, S_{55}, S_{66}, see Fig. 1) which are the ones of greatest interest when

*Since the preparation of this review, Dr P. B. Bowden died at Cambridge. His death is a great loss to materials science.
†Present address: Department of Engineering, University of Cambridge.

TABLE I Some elastic constants of polymer crystals. (All figures are in GN m^{-2} and those in italics are theoretical)

Type	Direction	C_{ik}	Polyethylene	Polyoxymethylene
Tensile moduli	Parallel to chain axis	C_{33}	240 [7], *256* [9], *325.4* [21]	150 [12]
	Perpendicular to chains	C_{11}	$3.2\left(\frac{1}{S_{11}}\right)$ [7], *4.83* [9], *13.7* [20], *13.75* [21]	2.5 [12]
		C_{22}	$3.9\left(\frac{1}{S_{22}}\right)$ [7], *8.71* [9], *11.9* [20], *12.50* [21]	$C_{22} = C_{11}$
Shear moduli	Parallel to chains	C_{44}	*2.83* [9], *31.9* [10], *3.5* [11], *3.19* [21]	~ 6 [12]
		C_{55}	*0.79* [9], *3.82* [10], *1.6* [11], *1.98* [21]	
	Perpendicular to chains	C_{66}	*2.06* [9], *6.24* [21]	

shear deformation processes such as slip, twinning and martensitic transformations are being considered. Some numerical values are given in Table I.

A similar situation applies to theoretical calculations. The tensile modulus in the chain direction can be readily estimated from the geometry of the chain and the force constants of the covalent bonds in the chain backbone [9]. Because of the covalent bonding such moduli are large (E_c = 256 GN m^{-2} for PE) although they are reduced slightly if the chain backbone is in a helical conformation [2] (E_c = 42 GN m^{-2} for monoclinic PP). Because the bonding between adjacent chains is only van der Waals or hydrogen bonding, the transverse tensile moduli and the shear moduli are almost two orders of magnitude smaller (see Table I). Such moduli are more difficult to calculate since it is necessary to choose appropriate interatomic potential functions and to compute for a chosen displacement the interaction between a number of atoms [9-11]. The discrepancies between calculated values in Table I highlight this point.

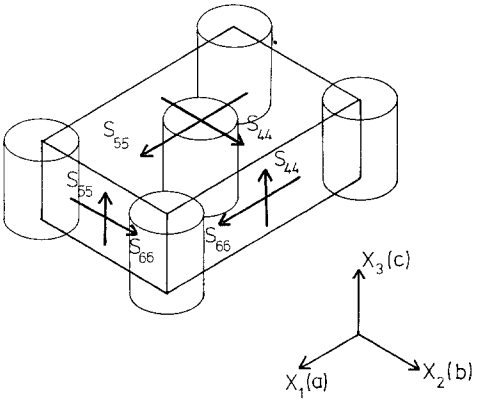

Figure 1 The PE unit cell (orthorhombic) showing the directions of the shear strains that define the three shear compliances, S_{44}, S_{55} and S_{66}. The principal axes for the elastic constants, x_1, x_2, x_3 coincide respectively with the *a*, *b* and *c* crystallographic axes.

3. The principles of the deformation of polymer crystals

3.1. The crystallography of slip

The plastic deformation of polymer crystals, like the plastic deformation of crystals of other materials, is generally expected to be crystallographic in nature and to take place without destroying the crystalline order. The only exception to this appears to be for the case of very large deformations when the crystals may be completely broken down and new crystals may form with no specific crystallographic relationship with the original structure [4].

Polymer crystals can deform plastically by slip, by twinning and by martensitic transformations, but the first of the three mechanisms is one of the more important ones since it is capable of producing larger plastic strains than the other two.

A *slip system* in a crystal is the combination of a *slip direction* and a *slip plane* containing that direction as shown in Fig. 2. A single slip system is only capable of producing a simple shear deformation of the crystal; for the crystal to undergo a general change of shape (as must occur in a deformed polycrystalline aggregate) *five independent* slip systems are necessary [6]. Polymer crystals rarely possess this number but under the right conditions deformation of bulk

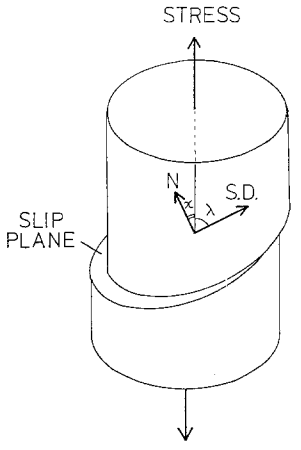

Figure 2 Single slip under a uniaxial tensile stress, σ. The slip-plane normal is N and S.D. is the slip direction. The resolved shear stress on the slip plane in the slip direction is given by $\tau = \sigma \cos \chi \cos \lambda$.

crystalline polymers without cracking or voiding still appears to be possible, perhaps because amorphous regions between adjacent crystals allow a certain amount of adjustment.

The slip plane is the crystallographic plane parallel to which slip takes place and in polymer crystals is restricted to a plane which contains the chain direction as the covalent bonds in the chain backbone remain unbroken during deformation. The slip direction is the direction in the slip plane in which slip takes place. A general principle that applies to the deformation of all crystalline materials is that the slip plane tends to be a close-packed plane in the structure and the slip direction a close-packed direction. In folded chain polymer crystals molecular folds at the surface of the crystal may in addition impose some restraint on the choice of slip plane since large amounts of slip will be able to occur only on planes parallel to the fold plane.

In metal crystals slip takes place when the resolved shear stress on the slip plane in the slip direction (see Fig. 2) reaches a critical value known as the critical resolved shear stress (CRSS). The value of the CRSS for metals is essentially independent of the hydrostatic component of the stress tensor or the normal stress on the slip plane. Work on the deformation of oriented crystalline polymers has shown that a similar criterion can sometimes be applied in the special case of well-annealed samples tested in compression [13]. If annealed samples are tested in tension or oriented samples are tested before annealing then the resolved shear stress for slip is not constant but increases markedly with increasing normal pressure on the slip plane [14-18].

An implication of the geometry of the slip process is that the orientation of a crystal undergoing single slip (that is a crystal in which only one slip system is active) will rotate relative to the stress axis. These rotations are illustrated in Fig. 3. For single slip the slip direction in the

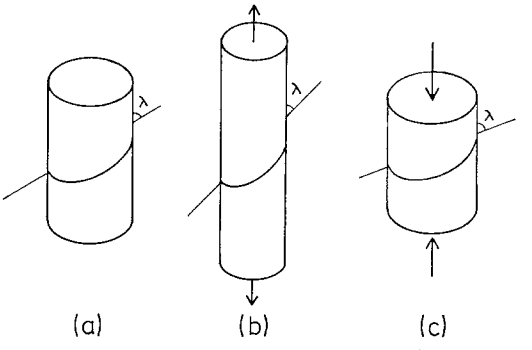

Figure 3 Rotations of a crystal undergoing single slip. (a) Undeformed crystal. (b) Uniaxial tension (λ decreases) and (c) Uniaxial compression (λ increases).

crystal always rotates directly *towards the direction of maximum extension*, that is it rotates towards the tensile axis in a test in uniaxial tension and directly away from the compression axis in a test in uniaxial compression. The angle through which the crystal rotates is a simple function of the applied strain [6].

When more than one slip system is operating at the same time the situation can be much more complicated [6, 19]. Two cases of particular interest when considering the deformation of polymer crystals are illustrated in Fig. 4. Fig. 4a illustrates a crystal in which there is a well-defined slip plane which becomes oriented perpendicular to the compression axis in a compression test. If slip in one direction occurs at a lower CRSS than slip in the other then it is this direction that will tend to become aligned in the direction of maximum extension in a test in uniaxial extension or plane strain extension since rotation due to slip in this direction will always occur first, before slip in the second direction causes the slip plane to rotate to become normal to the compression direction. In polymers, since the slip plane always contains the molecular chain axis which is generally a slip direction, two slip directions in a slip plane

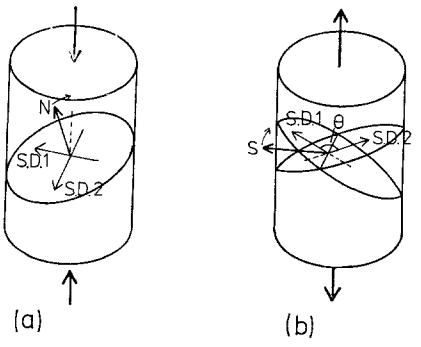

Figure 4 Situations in which there are two operating slip systems. (a) Slip plane containing two slip directions. The slip plane normal moves towards the compression axis in a compression test. (b) Two intersecting slip systems (see text). The vector sum of the slip directions in the acute angle, marked S in the figure, rotates towards the extension direction in a tension test.

are generally not crystallographically equivalent systems and, therefore, will have different CRSS's.

Fig. 4b illustrates a more complex case in which there are two crystallographically equivalent intersecting slip systems with the slip direction in each slip plane perpendicular to the line of intersection of the planes. The rotation that occurs depends on θ, the angle between the slip directions. If θ is not 90° then, if the crystal is in a general orientation, only one slip system will operate until the crystal has rotated to a symmetrical position with respect to the applied stress. At this point the resolved shear stress will be the same on both systems, both systems will operate together and *the vector sum of the slip directions in the acute angle* will rotate towards the direction of maximum extension. (If θ is 90° the resolved shear stress on both systems is the same for any applied stress, the direction of the vector sum becomes indeterminate, and the normal to the plane containing both slip directions will rotate away from the direction of maximum extension.)

3.2. Interpretation of the textures of oriented polymers

It is possible to obtain information about deformation mechanisms from the textures which develop during the deformation of crystalline polymers. In the interpretation of the textures several principles must be taken into account.

3.2.1. Resolved shear stress

The first consideration that can be used is that of resolved shear stress. Certain crystals will deform (i.e. rotate) before others because, owing to their particular orientation, the resolved shear stress on the slip plane in the slip direction is larger. In a polymer some crystals can deform before others because the amorphous material between the crystals can allow some relative motion. This consideration is only important in the early stages of deformation because at higher strains all crystals have to deform.

3.2.2. Uniaxial deformation

If the interactions between adjacent crystals are ignored the deformation mechanisms which give rise to the textures of specimens which have been deformed by either uniaxial extension or uniaxial compression are simple to determine using the considerations outlined in Section 3.1. In uniaxial extension for a crystal undergoing single slip the slip direction becomes aligned with the extension direction. In compression the slip directions become oriented radially about the compression direction. If slip can take place in two directions in one slip plane this will give rise to a texture with the slip plane perpendicular to the compression direction (cf. Section 3.1).

3.2.3. Plane strain deformation

Plane strain deformation is illustrated schematically in Fig. 5. A single crystal can only undergo

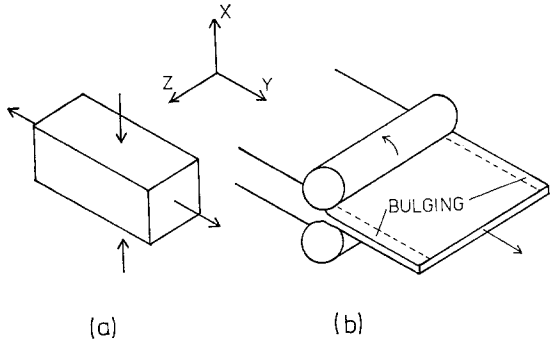

Figure 5 (a) Plane-strain deformation. There is no overall change in dimension in the z direction. (b) Rolling induces a plane strain deformation provided the sheet that is rolled is sufficiently wide for lateral bulging to be negligible.

this type of deformation if the slip direction lies in the plane strain plane. In this case, the slip direction should become aligned with the extension direction but provided the deformation is accurately plane strain there is no mechanism

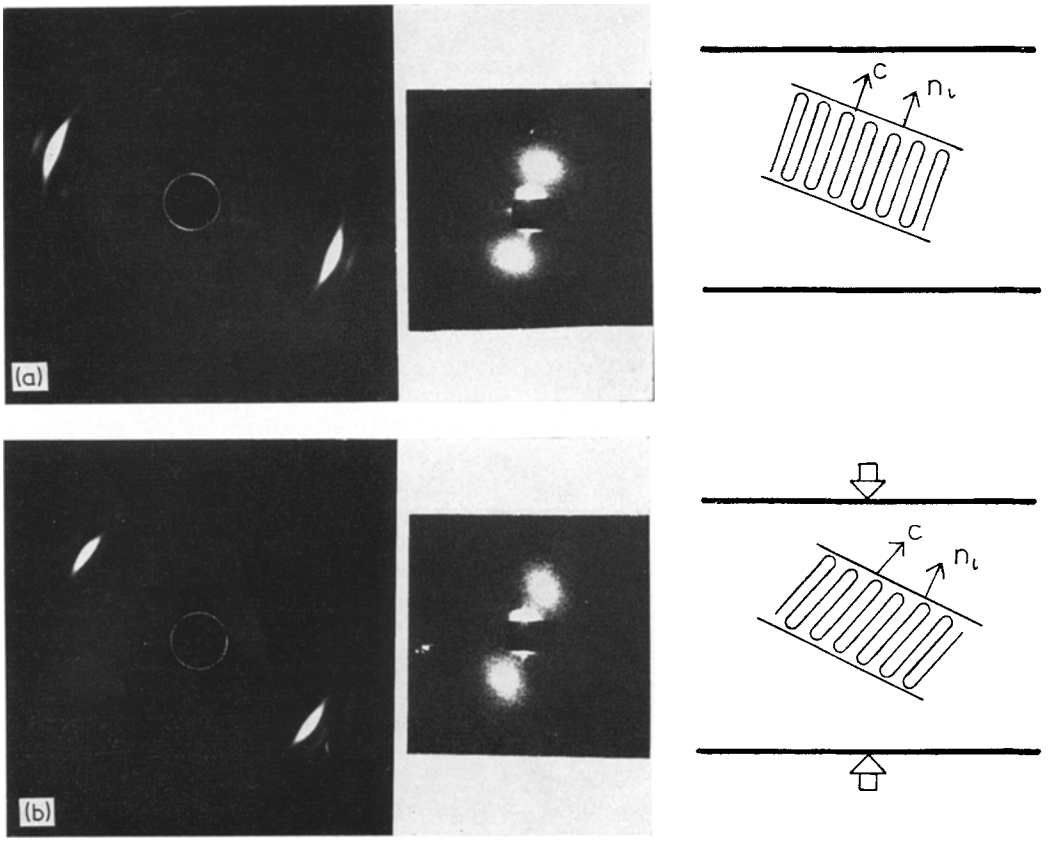

Figure 6 Wide- and small-angle X-ray diffraction patterns of a sample of HDPE with a single crystal texture with the X-ray beams parallel to ⟨100⟩. (a) Before deformation. (b) After deformation to a permanent plastic strain of 14%.

whereby the slip plane can rotate to become perpendicular to the compression direction. If the plane strain condition is relaxed and slip takes place in more than one direction in the slip plane then the slip plane rotates to become perpendicular to the compression direction as in the case of uniaxial compression shown in Fig. 4a.

In bulk crystalline polymers deformed by rolling for example, although the deformation of the sample as a whole may be plane strain, the deformation of an individual crystal in a general orientation cannot be so because polymers in general do not possess the five independent slip systems required for a general deformation. There must, therefore, be some degree of accommodation by mechanisms such as deforming the amorphous material, pushing the crystals apart or local cracking. It must also be noted that during rolling there is often significant bulging perpendicular to the plane strain plane (Fig. 5) particularly at higher strains. If a single slip system operates the slip direction will become aligned in the extension direction. For two slip systems sharing the same slip plane the plane will become oriented perpendicular to the compression direction and the slip direction with the lowest CRSS will tend to become oriented in the extension direction (see Section 3.1).

4. The deformation of polymer crystals

4.1. Slip in the chain direction

This type of deformation involves a translation of molecules past each other parallel to the chain direction [14]. The slip plane contains the chain direction (e.g. $\{hk0\}$ in PE) and the slip direction is parallel to the chain axis (⟨001⟩ in PE). The most common texture found after the deformation of nearly all crystalline polymers at sufficiently high draw ratios is the orientation of the crystals with the chain direction parallel to the draw direction. Following the considerations in Section 3.2.2 this is evidence for the deformation having taken place by chain slip as the slip direction is always expected to rotate towards the

tensile axis [6]. At high strains when most of the molecules are aligned parallel to the draw direction, crystals start to break up and reform in a new conformation [4]. Hansen and Rusnock [22] considered that chain direction slip was the process which controlled the natural draw ratios of crystalline polymers. However, more recent work [23] has shown that the draw ratio is controlled more strongly by factors such as the molecular weight which governs the number of tie molecules between crystals [24]. High molecular weights lead to high draw ratios.

From the analysis of the textures that are found after heavily deforming PE by plane strain deformation such as rolling [25] or compression-orientation [14] it is possible to show that both chain slip and transverse slip may operate simultaneously on a common slip plane. This type of deformation produces material with a texture of $\langle 001 \rangle$ parallel to the rolling direction and $\{100\}$ perpendicular to the compression direction. (The texture changes by twinning when the material is unloaded because of residual internal compressive stresses [26]). From the considerations of the analysis of texture in Section 3.2.3 this implies that the slip plane for both the chain slip and transverse slip is $\{100\}$ and that chain slip ($\{100\}\langle 001 \rangle$) has a lower CRSS than transverse slip. Chain direction slip has been suggested from observations upon the deformation of spherulites [27]. In the equatorial regions of PE spherulites where deformation takes place first of all, the crystal axis was found to rotate and this rotation appears to be easier around the *b*-axis than around *a*. This has been taken as an indication that $\{100\}\langle 001 \rangle$ slip is easier than $\{010\}\langle 001 \rangle$ slip [2] although it is not possible to rule out the possibility of deformation by lamella slip also giving rise to this observation [27].

It is possible to crystallize many polymers from dilute solution in the form of lamellae of the order of 100 Å thick [28]. The crystals may be deposited upon supporting films and examined in the electron microscope. It has been found by electron diffraction that the molecules are oriented approximately perpendicular to the lamella surfaces [29]. If they are deposited upon extensible substrates then when the substrate is extended the molecules may rotate and become tilted in the lamellae indicating deformation by chain slip [30]. However, if the molecules are accurately perpendicular to the substrate the resolved shear stress parallel to the molecules is zero and chain slip does not occur [31, 32]. Gleiter and Argon [33] suggested from the examination of slip traces on the surfaces of PE single crystals deformed upon a Cu single crystal substrate that $\langle 001 \rangle$ chain slip could take place on any $\{hk0\}$ plane. They also showed that chain slip was the only deformation activated at $-196°C$.

Chain direction slip has been found to be an important mechanism during the deformation of oriented crystalline polymers. A systematic study has been made of the deformation of drawn, rolled and annealed LDPE by Keller and his co-workers [26, 34-36]. Under certain circumstances it was found that the orientation of the molecules within the crystals changed and this was explained in terms of chain slip [35, 36]. From the specimen geometry the slip system was suggested to be $\{100\}\langle 001 \rangle$ [35]. Fig. 6 shows a set of small- and wide-angle X-ray diffraction patterns of HDPE with a well-defined single crystal texture, taken before and after deformation, by compression at an angle to the chain direction. After deformation the wide- and small-angle patterns diverge and the spots in the small-angle pattern shear over. This indicates that the orientation of the molecules within the crystals changes after deformation and from the deformation geometry the rotations are found to be consistent with $\{010\}\langle 001 \rangle$ chain slip [14, 37]. It has also been found that chain slip in PE takes place at a constant critical resolved shear stress of 15 ± 1 MN m^{-2} at 25°C. Recent work [37] has indicated that $\{100\}\langle 001 \rangle$ slip can also take place but at a lower CRSS of the order of 10 MN m^{-2}. Chain slip may also be highly reversible in LDPE [36] and HDPE [124] especially at higher temperatures.

Chain slip has been found to be a widespread deformation mechanism in polymers other than PE. Bulk PTFE is non-spherulitic and crystallizes in the form of thick lamella crystals up to 1 μm thick, and fracture-surface replicas examined in the electron microscope show striations parallel to the chain direction [38-40] as in Fig. 7a. When the material is deformed above room temperature (Fig. 7b) the striations which are initially parallel to the lamella surfaces become tilted [38, 39] and this has been taken as an indication of deformation by chain direction slip [40]. Drawn PTFE has a texture with $\langle 0001 \rangle$ parallel to the draw direction which is again consistent with deformation by chain slip [41]. From the analysis of the

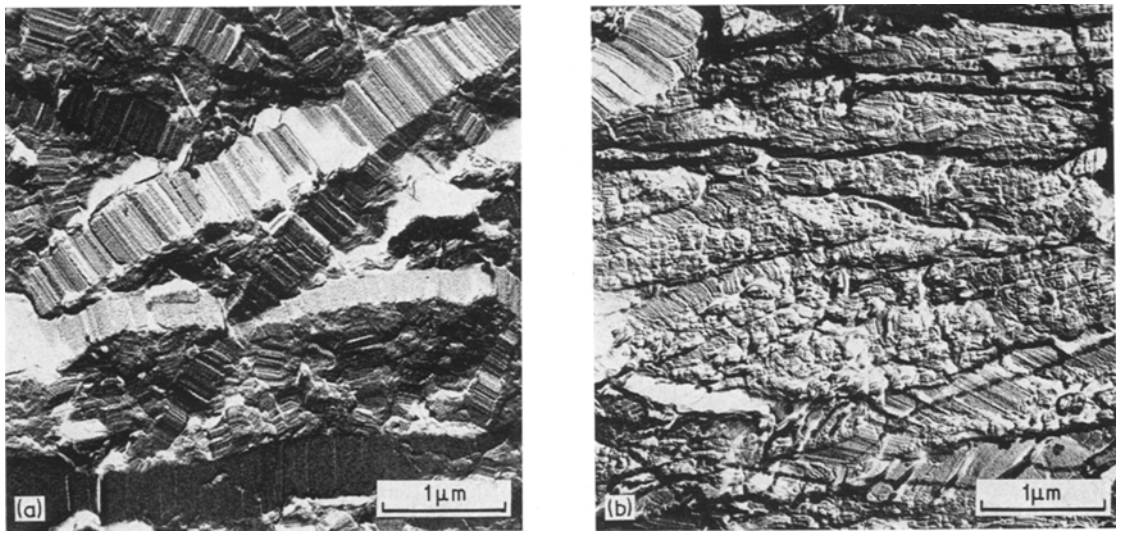

Figure 7 Electron micrographs of replicas of fracture surfaces of PTFE. (a) Before deformation. (b) After plane strain deformation at 20°C to a permanent plastic strain of 70%. The compression direction is vertical and the extension direction is horizontal.

textures of rolled polymers with hexagonal structures such as POM and PTFE [42-44] if it is assumed that transverse slip also may take place it is possible to determine the common slip plane. If they are rolled at high temperatures [42] a texture is developed with $\langle 0001 \rangle$ parallel to the rolling direction and $\{10\bar{1}0\}$, the closest packed plane, in the plane of the sheet. Using the considerations outlined in Section 3.2.3 this texture is consistent with chain slip and transverse slip taking place on the same plane and $\{10\bar{1}0\}$ $\langle 0001 \rangle$ chain direction slip being the easiest deformation mechanism. By rolling at lower temperatures a less well-defined texture is obtained [43, 44] and this is discussed in the section on transverse slip.

Kink bands are often found as the result of the deformation of oriented crystalline polymers such as PE [45-47], PP [48, 49] and nylon [50]. In all cases it has been found that the principal deformation mechanism involved in this type of deformation is chain direction slip and from the geometry of the kink bands it is often possible to determine the slip plane. Zaukelies [50] was able to show that kink bands in oriented nylon were due to chain direction slip on the hydrogen-bonded planes. Young [37] has also shown that chain direction slip in nylon 6 will only take place on the H-bonded planes. These are clear demonstrations of the strength of the hydrogen bonding within the sheets compared with the van der Waals bonding between sheets.

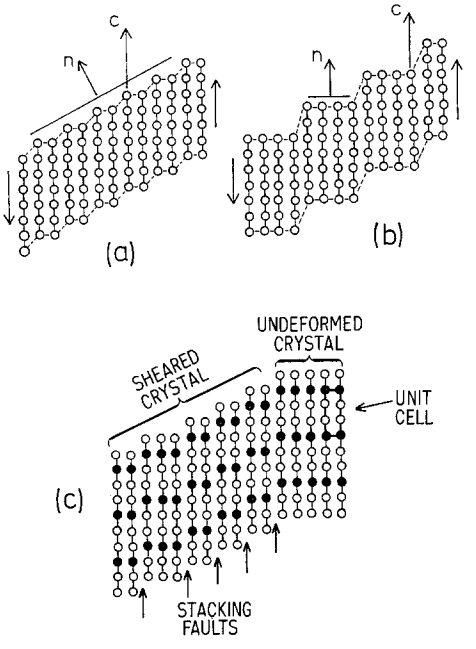

Figure 8 Schematic diagrams illustrating different degrees of fineness of slip. (a) Fine slip. A displacement of one lattice vector has occurred on every other lattice plane in the crystal. The direction n is the normal to the surface of the crystal which has rotated relative to the chain axis c during deformation. (b) Coarser slip. The same total shear has been produced by a displacement of two lattice vectors on every fourth plane. (c) Shearing of a lattice that has a large lattice vector in the chain direction by fine slip of partial dislocations.

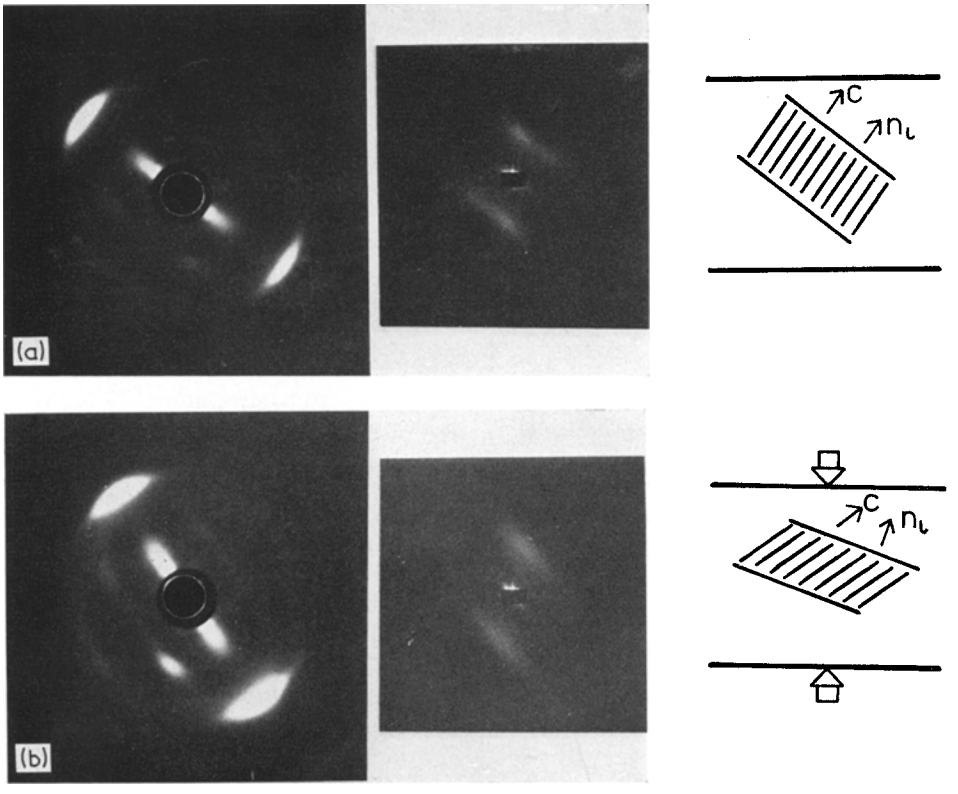

Figure 9 Wide- and small-angle X-ray diffraction patterns of a sample of oriented nylon 6. (a) Before deformation. (b) After deformation to a permanent plastic strain of 38% by compression at an angle of 37° to the chain direction (cf. Fig. 6 for PE). Note the shear of the spots in the wide-angle pattern.

4.2. Fine and coarse chain-direction slip; interfibrillar slip

Fig. 8a and b show schematically two crystals that have each deformed by single slip to the same final shear strain. In Fig. 8a (fine slip) a small amount of slip has occurred on a large number of planes; in Fig. 8b (coarse slip) larger amounts of slip have occurred on fewer planes. In polymers the modes can be distinguished since a wide-angle X-ray diffraction pattern indicates the direction of the chain axis, *c*, and a small-angle X-ray pattern indicates the direction of the lamella normal, *n*. For fine slip only *n* rotates relative to *c* whereas for coarse slip, which cannot be distinguished from interfibrillar slip [14] *n* and *c* rotate together and do not diverge.

In oriented and annealed samples of PE, slip can be relatively fine [14, 37] which is perhaps not surprising since the crystals are embedded in an amorphous rubbery matrix which will encourage affine deformation. In oriented samples of both PE and PP that have not been annealed there are small components of coarse or interfibrillar slip, due it has been suggested to the fibrous nature of the material [14, 18].

In polymer crystals with larger unit cells such as the nylons more complex effects can arise. In oriented and deformed samples of nylon 11 [51] and nylon 6 [37] the wide-angle diffraction pattern has been observed to become distorted. It has been suggested initially by Point *et al.* [51] that this is due to the shearing of the lattice by partial dislocations with Burgers vectors less than the lattice vector in the chain direction. The effect is illustrated schematically in Fig. 8c. The lattice vectors in the chain direction in nylons are large (15 to 20 Å) so the energies of dislocations with Burgers vectors equal to the lattice translation vector would be very large indeed. On the other hand, the energies of the stacking faults created by the partial dislocations would not be expected to be particularly high in nylon.

Fig. 9 illustrates the effect in nylon 6. The shear strain of 0.165 in the wide-angle pattern indicates a shear in the lattice of that magnitude in the opposite sense because of the reciprocal

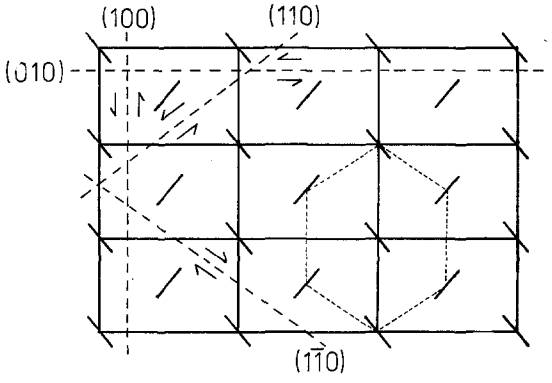

Figure 10 Transverse slip in PE. The unit cell is projected on {001}. The dotted hexagon becomes a regular hexagon when the molecules are not in the form of planar zig-zags but are helical as in PTFE.

relation between lattice and pattern. Such a shear corresponds to a displacement of one carbon zig-zag ($-CH_2-CH_2-$) between every fourth H-bonded plane.

4.3. Transverse slip

This type of deformation involves the sliding of molecules over each other in a direction perpendicular to the molecular axis. It is induced by a shear stress in a direction perpendicular to the chain axis and is illustrated for the case of PE in Fig. 10. The slip plane is again restricted to the type which contains the chain direction and the slip direction is of the type which is perpendicular to the chain direction.

The possible slip systems in PE have been considered by Frank *et al.* [52]. The closest-packed direction in Fig. 10 is ⟨010⟩ so this might be expected to be the easiest slip direction. ⟨100⟩ is the next longest. Since the {010} ⟨100⟩ slip system is orthogonal to {100} ⟨010⟩ the resolved shear stress on both systems will be the same so that {100} ⟨010⟩ will always be preferred. Slip on the third system in Fig. 10, {1$\bar{1}$0} ⟨110⟩, involves a large unit Burgers vector but the same authors have suggested that unit dislocations may be able to split into partial dislocations of the type ⟨$a/2$, $b/2$, γ⟩, ⟨$a/2$, $b/2$, $-\gamma$⟩. If γ is small they have shorter Burgers vectors than even ⟨010⟩ and so this might be expected to be an easy system. However, it is always in competition with {110} twinning modes and so may not be observed.

During the early stages of the drawing of both nylon [53] and PE [54] textures with the chain direction transverse to the draw direction have been found and they have been interpreted in terms of transverse slip [55]. The light rolling of isotropic PE is found to produce material with a poorly-defined texture of {100} planes in the plane of the sheet before there is any appreciable chain axis orientation. Frank *et al.* [52] showed that this was probably due to a combination of {100} ⟨010⟩ transverse slip and twinning. This is consistent with the ideas summarized in Section 3.2.3. If chain slip can occur at the same time as transverse slip there will be two slip systems acting in the {100} plane, {100} ⟨001⟩ and {100} ⟨010⟩, and the {100} plane will become oriented perpendicular to the compression direction.

From observations of slip steps on the surface of PE single crystals deformed on the surface of Cu single crystals, Gleiter and Argon [33] have suggested that both {100} ⟨010⟩ and {010} ⟨100⟩ transverse slip probably take place at room temperature but not at − 196°C.

When oriented HDPE with a *fibre* texture is compressed in a direction perpendicular to the chain axis it is found that {100} planes first of all rotate to become perpendicular to the compression direction. This has been explained in terms of twinning and {100} ⟨010⟩ transverse slip [56] (cf. [52]). When oriented HDPE with a *single crystal* texture is compressed in a direction between the *a*- and *b*-axes and perpendicular to *c* it is found that the *b*-axis rotates away from the compression direction and the *a*-axis (the normal to {100}) rotates towards the compression direction [37, 57]. From the analysis of single slip in Section 3.1 these rotations imply that deformation takes place by means of transverse slip on the {100} plane in the ⟨010⟩ direction. There is some evidence that {100} is the fold plane in bulk-crystallized samples of PE [58, 59]. Recently, Bevis and co-workers [60] by deforming PE single crystals on extensible substrates have found that transverse slip in PE can occur only on the fold plane ({110} in single crystals). Shear stresses on other planes are relieved by twinning and martensitic transformations (see Sections 4.4 and 4.5). The lath-shaped single crystals of PP tend to fracture when they are extended along their length which is ⟨010⟩ but do undergo plastic deformation when pulled in other directions. This observation has been explained by suggesting that transverse slip on {110} can take place [61].

In polymer crystals of hexagonal symmetry such as POM and PTFE the dotted hexagon in

Fig. 10 becomes a regular hexagon, slip systems on {100} and {110} in Fig. 10 become equivalent ({10$\bar{1}$0} planes in the hexagonal cell) and there are now three equivalent slip systems at 120° to each other. Gezovich and Geil [43] investigated the texture produced by cold-rolling POM and found that it was rather complex and could not be resolved without resorting to detailed pole figure analysis. They found that there was no maximum of {10$\bar{1}$0} poles normal to the rolling plane as in the hot-rolled material [42]. They did find maxima in the rolling plane transverse to and parallel to the rolling direction. They thought that slip in POM should take place on the closest packed plane {10$\bar{1}$0}, which should give rise to a texture with {10$\bar{1}$0} in the plane of the sheet (Section 3.2.3). However, if transverse slip is relatively easy, because of hexagonal symmetry it may occur on a pair of {10$\bar{1}$0} planes as explained in Section 3.1. In this situation the vector sum of the slip directions in the acute angle will become oriented in the extension direction and the pair of {10$\bar{1}$0} slip planes should become oriented at $\pm$ 30° to the plane of the sheet and parallel to the extension direction. It was pointed out in Section 3.2.3 that the plane strain condition within individual crystals may be relaxed and it was also found that above a 50% thickness reduction there was appreciable bulging [43]. This means that individual crystals probably extended both parallel and perpendicular to the rolling direction which would give rise to the texture with {10$\bar{1}$0} poles parallel and transverse to the rolling direction. Recent unpublished work [62] has shown that PTFE biaxially oriented at temperatures below room temperature has a texture similar to that of cold-rolled POM.

4.4. Twinning

Twinning may occur in polymer crystals if the crystal structure is of sufficiently low symmetry. Hexagonal metals normally twin readily on the basal plane but polymer crystals such as POM or PTFE which possess hexagonal symmetry cannot twin since the basal plane, {0001} is perpendicular to the chain axis. Bevis and Crellin [63] analysed twinning in PE crystals in detail. However, in simple terms the two basic twinning modes expected to occur are {310} and {110} twinning [52]. These two modes are illustrated in Fig. 11 with the unit cell projected upon {001}. {110} twinning produces a rotation of the lattice by 67° about ⟨001⟩

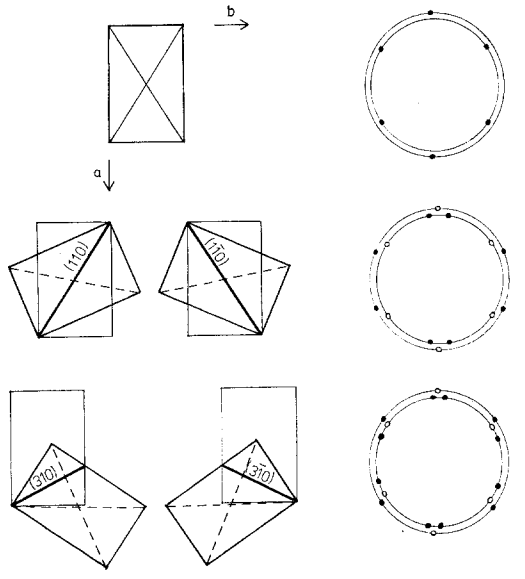

Figure 11 {110} and {310} twinning in orthorhombic PE with the unit cell projected on {001}. (After [52]). Schematic diagrams of the wide-angle X-ray diffraction patterns from the twinned and untwinned cells are also given. The open circles represent reflections from the untwinned cells.

whereas {310} twinning rotates the lattice by 55° about ⟨001⟩. Twinning modes in polymers have been identified either from traces of the habit plane in single crystals or from the rotations of the lattice. As the lattice is rotated about a particular crystallographic direction detailed investigations of twinning are usually carried out upon single crystals [31, 32] or polycrystalline specimens with a well-defined texture [56, 57]. However, care must be taken that there are no extra rotations because of slip.

The early evidence for twinning in PE was that it was found that during early stages of deformation or on unloading rotations occurred that were too large to be explained by slip alone [52, 64, 65]. Since the textures were not sufficiently well developed it was not possible to determine the exact twinning modes. Recent studies of heavily deformed PE using pole figures have lead to the unambiguous identification of these modes [25, 66]. The textures of drawn HDPE and LDPE are both consistent with {310} twinning but this remains the only strong evidence for this particular mode in PE. Other measurements upon single crystals and oriented material have lead to the identification of {110} twinning only.

Twinning has been found to be wide spread in

deformed single crystals of PE [31, 32] and Allen *et al.* [32] identified the mode as the {110} type. They had some evidence that {310} twinning took place within previously deformed {110} twins and also suggested that it was necessary for the fold plane to be {100} instead of {110} before {310} twinning could take place. The observation of {310} twinning on deforming bulk material [65, 66] lends support to the other evidence for {100} being the the fold plane of bulk PE [58, 59]. The irradiation of PE single crystals is found to depress all of the deformation mechanisms with the exception of {110} twinning [67]. Irradiation of polymers is known to introduce cross-linking and Andrews and Voigt-Martin [67] took this as an indication that cross-links between adjacent molecules inhibited slip and only permitted deformation modes such as twinning which require only small molecular displacements.

Seto *et al.* [56] found that when fibre textured PE was compressed in a direction transverse to the chain direction {100} planes became oriented perpendicular to the compression direction. The rotation of the lattice was too rapid to be explained by transverse slip alone so they suggested that twinning was also involved. They also noted that twinning was found on removing the applied compressive load (cf. Frank *et al.* [52]). More recent work [57] upon the deformation HDPE with a single crystal texture by compression in directions perpendicular to the chain direction has indicated that the twinning mode in oriented PE is the {110} type as in single crystals.

There is little detailed evidence for twinning in polymers other than PE. From the angles of kink bands observed in PP single crystals deformed to low strains twinning on {120} or {130} has been suggested [61] but there is no evidence for twinning in deformed POM single crystals (which is unlikely as it has a hexagonal crystal structure) or in nylon 6 single crystals [68]. Twinning, however, is found on the deformation of spherulitic nylon 66 [53, 71].

4.5. Stress-induced martensitic transformations

When bulk PE is deformed extra reflections appear in the wide-angle X-ray diffraction pattern indicating that the material has undergone a stress-induced phase change [69]. Oriented specimens with a well-defined texture [56, 57, 70] or single crystals [31, 32] are needed

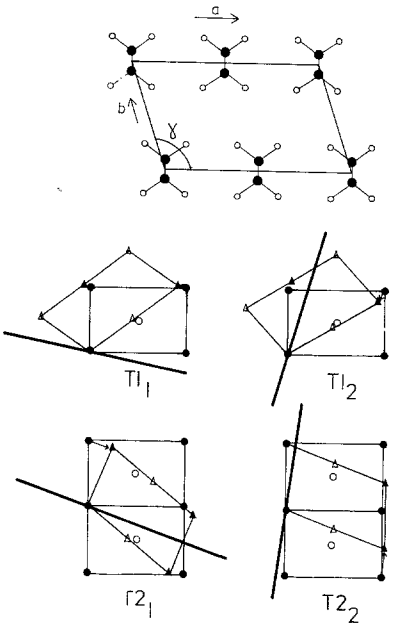

Figure 12 The monoclinic cell of PE projected on {001}. $a = 8.09$ Å, $b = 4.79$ Å, $c = 2.54$ Å, $\gamma = 107.9°$ [70]. The four transformation modes between the orthorhombic and monoclinic forms of PE, which involve the lowest shear strains, calculated by Bevis and Crellin [63] are also given.

in order to determine the structure of the new phase and its orientation relationship with the parent orthorhombic cell. Tanaka *et al.* [70] showed that when oriented PE was compressed in a direction perpendicular to the chain direction it underwent a stress-induced martensitic transformation to the monoclinic cell illustrated schematically in Fig. 12. Kiho *et al.* [31] later showed that an identical structure was produced by the deformation of single crystals. Bevis and Crellin [63] have predicted the orientation relationships between the two PE cells and the possible transformation modes by assuming that the monoclinic cell is formed by means of a simple shear deformation of the orthorhombic cell. The four modes involving the lowest shear strain are also given in Fig. 12. It has been found that there are two specific orientation relationships between the two cells in deformed PE single crystals and they correspond very closely to the 1_1 and 2_1 modes [32]. Measurements of the *initial* orientation relationship for the transformation in bulk material agree most closely with the relationship predicted for the 1_2 transformation [57, 71]. However, as the strain is increased the monoclinic cell is found to rotate,

by slip and twinning [56, 57], with respect to the orthorhombic cell and the orientation relationship then changes. The monoclinic cell also twins when the compressive load is removed [56, 57]. Repeated twinning of the monoclinic cell has been found in single crystals [72].

Kiho *et al.* [73] found that when deformed single crystals of PE were allowed to relax fully the monoclinic reflections disappeared and so they suggested that the monoclinic form of PE is a metastable phase and only present under stress. It has also been shown that the monoclinic cell is unstable above 110°C [74]. On annealing deformed PE single crystals it is found that crystals which previously exhibited {110} folding alter their fold plane to {100} [75]. This has been taken as an indication that the monoclinic phase may be an intermediate step in the fold-plane transition. The difference between the fold plane of bulk PE and that of single crystals may also help to explain why different modes are found in the two forms of the same material.

No evidence for a similar transformation in deformed POM or nylon single crystals has been found [68, 76].

4.6. Dislocations in polymer crystals

Early predictions of dislocations in polymer crystals [88] were made from the discontinuity of Moiré fringes between slightly mis-oriented overlapping PE single crystals observed in the electron microscope [28, 77, 78]. The first direct observation of dislocations in PE was made by Petermann and Gleiter [79] who observed contrast in dark-field electron micrographs of single crystals which they interpreted as being due to screw dislocations with Burgers vectors parallel to the chain direction and they tentatively described these dislocations as being responsible for chain direction slip (cf. [125].)

Attempts have been made to describe the structure of crystalline polymers in terms of a crystal defect model [50, 80-82]. Predecki and Statton [80] proposed that crystalline polymers were essentially 100% crystalline but that defects such as chain-ends or chain-folds were incorporated in the lattice reducing the crystallinity as measured by density or X-ray diffraction. They considered several distributions of defects within the lattice in terms of dislocations and in a later publication [81] went on to show how these dislocations might be associated with deformation by transverse slip. Although some defects may be incorporated in crystalline regions it has been shown that, at least in single crystals of PE, only about 10% of chain ends are situated within the crystal lattice [83].

The yield stresses of crystals are governed either by the generation of dislocations or the Peierls stress required to move them. There has been a number of papers that have interpreted successfully the stress-strain-strain-rate behaviour of polymers in terms of the generation and propagation of dislocations [84-86]. The equations they used were derived for dislocation propagation in large crystals and they tended to ignore the possible limitations imposed on dislocation propagation by the special morphology of crystalline polymers. Because polymer crystals may be only of the order of about 200 Å thick, Peterson [87] has suggested that screw dislocations with Burgers vectors along the chain direction might be generated thermally under the action of an applied shear stress. Such a process is reasonable in polymer crystals because they have small shear moduli (Table I) and are relatively thin. Peterson [10] has also calculated the Peierls stress needed to move such dislocations, once formed, through the PE lattice. The calculation depends upon rather unreliable calculated values of shear moduli (Section 2). However, the results indicated that {100}⟨001⟩ slip by dislocation motion should be very much easier than {010}⟨001⟩ slip. This is consistent with the observations in Section 4.1 that chain direction slip on {100} is easier than that upon {010} [37].

5. Deformation of the amorphous phase

The interpretation of the deformation of the amorphous phase in crystalline polymers depends upon the model that is chosen to describe the structure. There is not yet full agreement on this structure and this sometimes gives rise to difficulties in envisaging details of some of the deformation mechanisms that have been proposed.

The two-phase model for bulk-crystallized polymers (e.g. [29]) is now generally accepted although there is still some support for the crystal defect model [50, 80-82]. It is now thought that the material consists of lamella crystals, not unlike those grown from dilute solution, which are separated from each other by amorphous polymer and are to some extent held together by tie molecules through the amorphous phase [29]. Oriented crystalline polymers have been described in a similar way with the crystals arranged

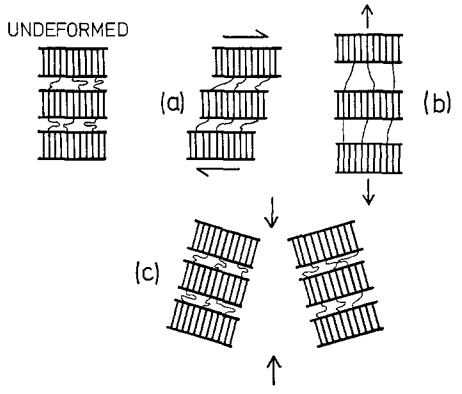

Figure 13 Deformation of the amorphous phase. (a) Interlamellar slip (or shear). (b) Interlamella separation. (c) Stack rotation.

in stacks [89] or as parallel wavy lamellae [90] separated by amorphous material and again held together by tie molecules. Recently there has been some support for the idea that oriented polymers are made up of a classical two-phase amorphous-crystalline component and another distinct phase similar to that described by the crystal defect model [88], although there is little direct morphological evidence to support it.

There is evidence that the non-crystalline material is discrete and displays the characteristics of an amorphous polymer such as undergoing a glass-transition [91, 92]. However, the properties of the material in an amorphous-crystalline matrix may be different from those of amorphous material in isolation.

Deformation mechanisms in the amorphous phase are most clearly demonstrated in specially prepared and well-characterized samples using a combination of small- and wide-angle X-ray diffraction and this is how most of the evidence in this section has been obtained.

5.1. Interlamella slip

This mechanism involves the shear of the lamella crystals parallel to each other with the amorphous phase undergoing a simple shear deformation. It is illustrated schematically in Fig. 13a and should be a relatively easy mechanism above the T_G when the amorphous phase may be expected to behave like a rubber and shear at a relatively low stress.

Using X-ray diffraction it has been possible to show that interlamella slip is an important mechanism during the deformation of PE. Keller and his co-workers [26, 34-36] employing a combination of small- and wide-angle X-ray diffraction found that interlamella slip occurred during the deformation of drawn, rolled and annealed LDPE both at and above room temperature and suggested that it was the principal deformation mechanism above 80°C [36]. The difference between the structure of hot- and cold-drawn LDPE has also been explained by greater amounts of interlamellar slip occurring at higher temperatures [93]. It is possible to prepare HDPE with a good texture and a well-defined lamella crystal structure [59] and an investigation of the deformation of this material at various angles to the chain direction using a combination of small- and wide-angle X-ray diffraction has shown that the elastic part of the deformation can be almost entirely accounted for by reversible interlamella slip [14]. The reversibility of interlamella slip is consistent with our ideas of polymer morphology as the tie molecules between the crystals should become extended on deformation and so should tend to pull the crystals back to their original positions when the stress is relaxed.

It is possible to observe permanent lamella slip in polymers by comparing replicas of specimens of spherulitic PE in the electron microscope before and after deformation. Predecki and Thornton [94] found that close to the melting point deformation took place mainly by slip between lamellae and they related this to the α' relaxation which is found at similar temperatures and has been attributed to a similar mechanism [3]. Lamella slip within PE spherulites has also been observed by Kobayashi and Nagasaura [95] close to the melting point and by Nakafuku *et al.* [96] during creep experiments.

5.2. Interlamella separation

Keller and Pope [36] found that when oriented LDPE with a well-defined lamellae crystal structure was compressed or stretched parallel to the orientation direction the change in the small-angle X-ray long period with the specimens still under load could be explained by a change in the interlamellar separation. This mechanism is illustrated schematically in Fig. 13b and should be induced by a component of tension or compression parallel to the lamellar surface.

If the amorphous phase behaved like a perfect rubber this type of deformation should be difficult since on the conventional model of the structure the amorphous material is in effect held between two semi-infinite plates. Any

change in the interlamella separation could not, therefore, be accompanied by a sideways contraction and so the deformation should involve a change in volume. Rubbers tend to have high bulk moduli and relatively low shear moduli and so should be resistant to volume changes. The fact that significant changes in the interlamella spacing occur implies that the lamellae are very thin in a direction perpendicular to the page in Fig. 13 or that a very different model is needed to describe the structure [121]. Hard elastic fibres are found to deform primarily by the formation of voids between lamellae [122] and a reduction in the density of the amorphous layers has been observed on stretching oriented polymers [123].

5.3. Stack rotation

This type of deformation is illustrated schematically in Fig. 13c and postulates a specific model for the structure of crystalline polymers. It is necessary that the lamellae are in the form of a stack which is free to rotate under the action of an applied stress and that the stack is surrounded by amorphous material which is able to take up any distortions caused by deformation. The possibility of the lamella stacks being surrounded by soft amorphous material has been suggested [97] from observations upon the deformation of LDPE with a well-defined lamella crystal structure [34]. It was found that the change in the periodicity of the lamella stacks as measured by small-angle X-ray diffraction was less than that calculated from the macroscopic strain applied to the specimens.

Groves and Hirsch [97] suggested the possibility of stack rotation as an alternative explanation of the changes in the small- and wide-angle X-ray diffraction patterns of oriented LDPE obtained before and after deformation by Cowking and co-workers [34]. The changes had been interpreted in terms of interlamella slip but Groves and Hirsch showed that stack rotation was possibly a better explanation of the X-ray data.

6. The deformation of bulk-crystallized polymers

6.1. Deformation of spherulites

Early theories of the deformation of semi-crystalline polymers such as the floating-rod model of Kratky [98] assumed that the orientation of the crystals after deformation could be explained by randomly oriented crystals

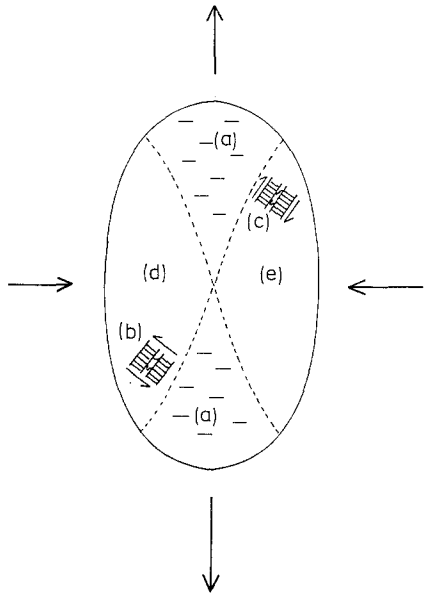

Figure 14 Schematic diagram of the plane strain deformation of a two-dimensional spherulite. Possible deformation mechanisms are indicated. (a) Cracking in azimuthal sectors [110]. (b) Chain direction slip. (c) Interlamella slip. (d) Twinning or martensitic transformations. (e) Transverse slip.

embedded in a continuous matrix undergoing an affine deformation. Although such theories did predict chain axis orientation they were unable to predict the deformation behaviour in detail.

A major advance was made by Wilchinsky [99] who considered the existence of crystals in the form of spherulites and accounted for their re-orientation in terms of the deformation of spherulites. This idea has been elaborated by Stein and co-workers [100, 101] and others [102-104] who have incorporated many of the deformation mechanisms discussed in Sections 4 and 5 into various models to describe spherulite deformation.

Hay and Keller [27] observed the deformation of spherulitic LDPE film using optical microscopy and found that the response of the spherulites to deformation (both elastic and plastic) was non-uniform and highly recoverable. Deformation was found to take place first of all in spherulite radii perpendicular to the draw-direction as illustrated in Fig. 14. At higher draw ratios the whole of the spherulite was found to deform and eventually a fibre structure was produced. The structural changes associated with the deformation of isotactic PP have been discussed by Samuels [105]. As the deforma-

tion proceeds the spherulites are found to become elongated parallel to the draw-direction. Eventually the lamella crystals start to break up and the material takes on a fibre structure. It is evident at this stage that some reformation of crystals takes place as the long period of the fibre structure has been found by Peterlin and Baltá-Calleja [106-108] to be independent of the original long period. The deformation of PP spherulites has been shown to depend upon the thermal history of the specimens and the nature of the spherulites [109, 110]. Spherulites grown at low temperatures tend to form microcracks in sectors parallel to the draw direction possibly because they contain tangential lamellae and cracks form on planes of weakness between the lamellae [110]. Those grown at higher temperatures deform affinely since they have radial lamellae like PE.

Deformation of the non-crystalline interspherulitic material is thought to occur because the measured draw-ratio of nylon 66 spherulites may be less than that of the samples as a whole [111]. However, in other polymers such as PP it is possible to obtain excellent agreement between the draw-ratio of the spherulites and that of the specimen [112].

In general, it is found that the exact nature of the deformation of spherulites is extremely temperature-dependent [93-96]. By examining surface replicas of deformed PE spherulites in the electron microscope Predecki and Thornton [94] were able to show that at $-20°$ the deformation was confined to the areas between spherulites. When the temperature was raised the deformation was found to be almost entirely within the lamella crystals and close to the melting point slip between the lamellae was found to become an important mechanism.

6.2. The strength of bulk-crystallized polymers

The strength of crystalline polymers varies both with polymer morphology and the testing conditions. The yield stress depends strongly upon the strain-rate and temperature of the test [85] and the hydrostatic pressure [113, 114]. Even if these variables are held constant the strength of any one polymer depends also upon the morphology and thermal history of the sample. The annealing of HDPE increases the yield stress (Fig. 15) but if it is strongly annealed under pressure (< 3 kbar) to extended chain crystals it becomes brittle probably because of

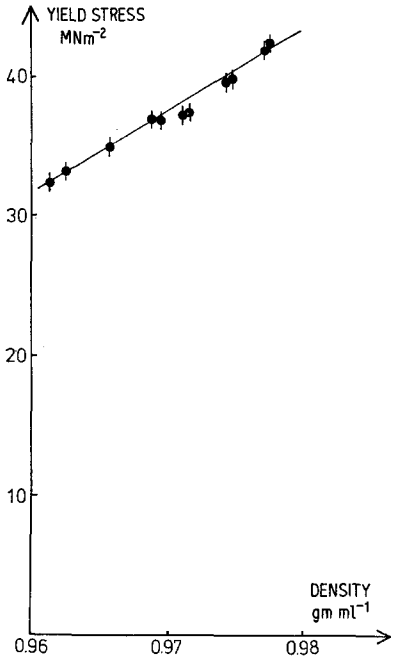

Figure 15 The plane strain compressive yield stress of HDPE as a function of specimen density. 0.96 g ml^{-1} corresponds to a degree of crystallinity of about 71% and 0.98 g ml^{-1} corresponds to one of about 86%.

the lack of intercrystalline links [115]. It is not really clear why the yield stress increases with annealing. The crystallinity increases and this in itself should increase the strength on a simple composite model [116]. However, the lamella thickness also increases although there is no evidence for correlating lamellar thickness alone with yield stress. Andrews [117] has developed a theory of yield in crystalline polymers involving the breaking of the points of contact between lamellae at yield. The probability of lamellae touching increases with crystallinity and the increase in contact area then raises the stress required for yield. Starkweather and Brooks [118] showed that the yield stress of nylon 66 increased as the spherulite size was reduced. They related this to the increase in yield stress in metals as the grain size is reduced (e.g. [119]). Any analogy between grains in metals, which are essentially single crystals, and spherulites, which are aggregates of polymer crystals would seem to be very doubtful. Care must be taken in the intepretation of such effects in polymers since the variation of spherulite size is usually obtained

by employing different heat treatments and these can also change other important variables such as crystallinity and crystal size, which may also affect the yield stress [117].

The strength of polymers also depends upon the state of the amorphous phase. For example, dry nylon 6 at 20°C yields at 70 MN m^{-2} whereas when the amorphous material is plasticized by water the yield stress is reduced to 40 MN m^{-2} (cf. PE 35 MN m^{-2}).

There is no strong dependence of the yield stress of isotropic PE upon molecular weight but other mechanical properties such as natural draw-ratio may be affected [23]. If the molecular weight is reduced there are usually fewer intercrystalline links [24] and this causes the notch sensitivity to be increased. Both the coefficient of friction and the rate of wear are found to be lower for very high molecular weight material [120].

References

1. A. PETERLIN, *Ann. Rev. Mat. Sci.* **2** (1972) 349.
2. R. P. KAMBOUR and R. E. ROBERTSON, in "Polymer Science" (edited by A. D. Jenkins) (North-Holland, London, 1972).
3. N. G. MCCRUM, B. E. READ and G. WILLIAMS, "Anelastic and Dielectric Effects in Polymeric Solids" (John Wiley, London, 1967).
4. A. PETERLIN, *J. Mater. Sci.* **6** (1971) 490.
5. L. HOLLIDAY and J. W. WHITE, *Pure and Appl. Chem.* **26** (1971) 545.
6. A. KELLY and G. W. GROVES, "Crystallography of Crystal Defects" (Longman, London, 1970).
7. I. SAKURADA, T. HO and K. NAKAMAE, *J. Polymer Sci.* **C15** (1966) 75.
8. J. W. WHITE, in "Polymer Science" (edited by A. D. Jenkins) (North-Holland, London, 1972).
9. A. ODAJIMA and T. MAEDA, *J. Polymer Sci.* **C15** (1966) 55.
10. J. M. PETERSON, *J. Appl. Phys.* **39** (1968) 4920.
11. R. L. MCCULLOUGH and J. M. PETERSON, *ibid* **44** (1973) 1224.
12. J. W. WHITE, private communication.
13. P. B. BOWDEN and R. J. YOUNG, *Nature Phys. Sci.* **229** (1971) 23.
14. R. J. YOUNG, P. B. BOWDEN, J. RITCHIE and J. G. RIDER, *J. Mater. Sci.* **8** (1973) 23.
15. A. KELLER and J. G. RIDER, *ibid* **1** (1966) 389.
16. T. HINTON and J. G. RIDER, *J. Appl. Phys.* **39** (1968) 4932.
17. L. A. SIMPSON and T. HINTON, *J. Mater. Sci.* **6** (1971) 558.
18. D. SHINOZAKI and G. W. GROVES, *ibid* **8** (1973) 1012.
19. D. K. BOWEN and J. W. CHRISTIAN, *Phil. Mag.* **12** (1965) 369.
20. D. E. WILLIAMS, *J. Chem. Phys.* **47** (1967) 4680.
21. C. WOBSER and S. BLASENBREY, *Kolloid Z. u. Z. Polymere* **241** (1970) 985.
22. D. HANSEN and J. A. RUSNOCK, *J. Appl. Phys.* **36** (1965) 332.
23. J. M. ANDREWS and I. M. WARD, *J. Mater. Sci.* **5** (1970) 411.
24. R. G. VADIMSKY, H. D. KEITH and F. J. PADDEN, *J. Polymer Sci.* A-2 **7** (1969) 1367.
25. D. LEWIS, E. J. WHEELER, W. F. MADDAMS and J. E. PREEDY, *ibid* **10** (1972) 369.
26. I. L. HAY and A. KELLER, *J. Mater. Sci.* **2** (1967) 538.
27. *Idem, Kolloid Z. u. Z. Polymere* **204** (1965) 43.
28. P. H. GEIL, "Polymer Single Crystals" (Interscience, New York, 1963).
29. A. KELLER, *Rep. Prog. Phys.* **31** (1968) 623.
30. H. KIHO, A. PETERLIN and P. H. GEIL, *J. Polymer Sci.* **B3** (1965) 257.
31. *Idem, J. Appl. Phys.* **35** (1964) 1599.
32. P. ALLAN, E. B. CRELLIN and M. BEVIS, *Phil. Mag.* **27** (1973) 127.
33. H. GLEITER and A. ARGON, *ibid* **24** (1971) 71.
34. A. COWKING, J. G. RIDER, I. L. HAY and A. KELLER, *J. Mater. Sci.* **3** (1968) 646.
35. A. COWKING and J. G. RIDER, *ibid* **4** (1969) 1051.
36. A. KELLER and D. P. POPE, *ibid* **6** (1971) 453.
37. R. J. YOUNG, Ph.D. Thesis, "Deformation Mechanisms in Crystalline Polymers" (University of Cambridge, 1972).
38. C. J. SPEERSCHNEIDER and C. H. LI, *J. Appl. Phys.* **33** (1962) 1871.
39. *Idem, ibid* **34** (1963) 3004.
40. S. SHERRATT, *Encylo. Chem. Tech.* **9** (1966) 805.
41. S. M. WECKER, T. DAVIDSON and D. W. BAKER, *J. Appl. Phys.* **43** (1972) 4345.
42. R. W. GRAY and N. G. MCCRUM, *Nature Phys. Sci.* **234** (1971) 117.
43. D. M. GEZOVICH and P. H. GEIL, *J. Mater. Sci.* **6** (1971) 509.
44. J. E. PREEDY and E. J. WHEELER, *Nature Phys. Sci.* **60** (1972) 236.
45. M. KUROKAWA and T. BAN, *J. Appl. Polymer Sci.* **8** (1964) 971.
46. T. SETO and Y. TAJIMA, *Japan. J. Appl. Phys.* **5** (1966) 354; Y. TAJIMA, *ibid* **12** (1973) 40.
47. A. KELLER and J. G. RIDER, *J. Mater. Sci.* **1** (1966) 389.
48. R. E. ROBERTSON, *J. Polymer Sci.* A-2 **7** (1969) 1315.
49. *Idem, ibid* **9** (1971) 1255.
50. D. A. ZAUKELIES, *J. Appl. Phys.* **33** (1962) 2797.
51. J. J. POINT, M. DOSIÈRE, M. GILLIOT and A. GOFFIN-GÉRIN, *J. Mater. Sci.* **6** (1971) 479.
52. F. C. FRANK, A. KELLER and A. O'CONNOR, *Phil. Mag.* **3** (1958) 64.
53. A. KELLER, *J. Polymer Sci.* **21** (1956) 363.
54. *Idem, ibid* **15** (1955) 31.

55. P. PREDECKI and W. O. STATTON, *J. Appl. Phys.* **38** (1967) 4140.
56. T. SETO, T. HARA and T. TANAKA, *Japan J. Appl. Phys.* **7** (1968) 31.
57. R. J. YOUNG and P. B. BOWDEN, *Phil. Mag.* **29** (1974) 1061.
58. M. I. BANK and S. KRIMM, *J. Polymer Sci.* A-2 **7** (1969) 1785.
59. R. J. YOUNG and P. B. BOWDEN, *J. Mater. Sci.* **8** (1973) 1177.
60. P. ALLAN and M. BEVIS, private communication.
61. P. CERRA, D. R. MORROW and J. A. SAUER, *J. Macromol. Sci.* **B3** (1969) 33.
62. R. J. YOUNG, *Polymer*, to be published.
63. M. BEVIS and E. B. CRELLIN, *Polymer* **12** (1971) 666.
64. A. PETERLIN, *J. Polymer Sci.* **C15** (1966) 427.
65. *Idem, ibid* **C18** (1967) 123.
66. D. LEWIS, E. J. WHEELER, W. F. MADDAMS and J. E. PREEDY, *J. Appl. Cryst.* **4** (1971) 55.
67. E. H. ANDREWS and I. G. VOIGT-MARTIN, *Proc. Roy. Soc.* A **327** (1972) 251.
68. P. H. GEIL, *J. Polymer Sci.* **A2** (1964) 3857.
69. W. P. SLICHTER, *ibid* **21** (1956) 141.
70. K. TANAKA, T. SETO and T. HARA, *J. Phys. Soc., Japan* **17** (1962) 873.
71. I. L. HAY and A. KELLER, *J. Polymer Sci.* **C30** (1970) 289.
72. P. H. GEIL, H. KIHO and A. PETERLIN, *ibid* **B2** (1964) 71.
73. H. KIHO, A. PETERLIN and P. H. GEIL, *ibid* **B3** (1965) 157.
74. *Idem, ibid* **B3** (1965) 263.
75. Y. KIKUCHI and S. KRIMM, "Plastic Deformation of Polymers" (edited by A. Peterlin) (Marcel Dekker, New York, 1971).
76. C. A. GARBER and P. H. GEIL, *Makromol. chem.* **113** (1968) 251.
77. V. F. HOLLAND, *J. Appl. Phys.* **35** (1964) 1351.
78. *Idem, ibid* **35** (1964) 3235.
79. J. PETERMANN and H. GLEITER, *J. Mater. Sci.* **8** (1973) 673.
80. P. PREDECKI and W. O. STATTON, *J. Appl. Phys.* **37** (1966) 4053.
81. *Idem, ibid* **38** (1967) 4140.
82. J. J. POINT, M. DOSIÈRE, M. GILLIOT and A. GOFFIN-GÉRIN, *J. Polymer Sci.* **C38** (1972) 261.
83. A. KELLER and D. J. PRIEST, *ibid* **B8** (1970) 1.
84. B. N. DEY, *J. Appl. Phys.* **38** (1967) 4144.
85. B. W. CHERRY and P. L. MCGINLEY, *Appl. Polymer Symp.* **17** (1971) 59.
86. *Idem, J. Macromol. Sci.-Chem.* **A6** (1972) 811.
87. J. M. PETERSON, *J. Appl. Phys.* **37** (1966) 4047.
88. M. L. WILLIAMS, *Ann. New York Acad. Sci.* **155** (1969) 539.
89. I. L. HAY and A. KELLER, *J. Mater. Sci.* **1** (1966) 41.
90. M. J. HILL and A. KELLER, *J. Macromol. Sci.-Phys.* **B5** (1971) 591.
91. G. T. DAVIS and R. K. EBY, *J. Appl. Phys.* **44** (1973) 4247.
92. E. S. FISCHER and F. KLOOS, *J. Polymer Sci.* **B8** (1970) 685.
93. B. H. MCCONKEY, M. W. DARLINGTON, D. W. SAUNDERS and C. G. CANNON, *J. Mater. Sci.* **6** (1971) 572.
94. P. PREDECKI and A. W. THORNTON, *J. Appl. Phys.* **41** (1970) 4342.
95. K. KOBAYASHI and T. NAGASAURA, *J. Polymer Sci.* **C15** (1966) 163.
96. C. NAKAFUKU, K. MINATO and T. TAKEMURA, *Japan J. Appl. Phys.* **7** (1968) 1155.
97. G. W. GROVES and P. B. HIRSCH, *J. Mater. Sci.*, **4** (1969) 929.
98. D. KRATKY, *Kolloid Z.* **84** (1938) 149.
99. Z. W. WILCHINSKY, *Polymer* **5** (1964) 271.
100. K. SASAGURI, S. HOSHINO and R. S. STEIN, *J. Appl. Phys.* **35** (1964) 47.
101. K. SASAGURI, R. YAMADA and R. S. STEIN, *ibid* **35** (1964) 3188.
102. T. ODA, N. SAKAGUCHI and H. KAWAI, *J. Polymer Sci.* **C15** (1966) 223.
103. S. NOMURA, A. ASANUMA, S. SUEHIRO and H. KAWAI, *ibid* **A-2 9** (1971) 1991.
104. S. NOMURA, M. MATSUO and H. KAWAI, *J. Polymer Sci., Polymer Phys. Edition*, **10** (1972) 2489.
105. R. J. SAMUELS, "Plastic Deformation of Polymers" (edited by A. Peterlin) (Marcel Dekker, New York, 1971).
106. A. PETERLIN and F. J. BALTÁ-CALLEJA, *J. Appl. Phys.* **40** (1969) 4238.
107. F. J. BALTÁ-CALLEJA and A. PETERLIN, *J. Mater. Sci.* **4** (1969) 722.
108. *Idem*, "Plastic Deformation of Polymers" (edited by A. Peterlin) (Marcel Dekker, New York, 1971).
109. J. L. WAY and J. R. ATKINSON, *J. Mater. Sci.* **6** (1971) 102.
110. *Idem, ibid* **7** (1972) 1345.
111. R. G. CRYSTAL and D. HANSEN, *J. Polymer Sci.* **A-2 6** (1968) 981.
112. R. J. SAMUELS, *ibid* **C13** (1966) 37.
113. D. R. MEARS, K. D. PAE and J. A. SAUER, *J. Appl. Phys.* **40** (1970) 4229.
114. A. W. CHRISTIANSEN, E. BAER and S. V. RADCLIFFE, *Phil. Mag.* **24** (1971) 451.
115. D. C. BASSETT and D. R. CARDER, *ibid* **28** (1973) 535.
116. J. C. HALPIN and J. L. KARDOS, *J. Appl. Phys.* **43** (1972) 2235.
117. E. H. ANDREWS, *Pure and Applied Chem.* **31** (1972) 91.
118. H. STARKWEATHER and R. E. BROOKS, *J. Appl. Polymer Sci.* **1** (1959) 236.
119. N. J. PETCH, *J. Iron Steel Inst.* **173** (1953) 25.
120. C. M. POOLEY and D. TABOR, *Proc. Roy. Soc.* **A239** (1972) 251.
121. R. G. C. ARRIDGE, *J. Mater Sci.* **9** (1974) 155.

122. R. G. QUYNN and H. J. BRODY, *J. Macromol. Sci.* **B5** (1971) 721.
123. V. S. KUKSENKO and A. I. SLUTSKER, *Sov. Phys. (Solid State)* **10** (1968) 657.
124. M. YAMADA, K. MIYASAKA and K. ISHIKAWA, *J. Polymer. Sci.* **A-2 9** (1971) 1083.
125. R. J. YOUNG, *Phil. Mag.* **30** (1974) 85.

Received 22 March and accepted 21 May 1974.